Neurobiology of Aging 73 (2019) 41–49

Contents lists available at ScienceDirect

Neurobiology of Aging

journal homepage: www.elsevier.com/locate/neuaging

miR-125b promotes tau phosphorylation by targeting the neural cell adhesion molecule in neuropathological progression

Linyu Zhang [a], Hao Dong [a], Youwen Si [a], Nan Wu [a], Hao Cao [b], Bing Mei [a,**], Bo Meng [a,*]

[a] Key Laboratory of Brain Functional Genomics, Ministry of Education, Shanghai Key Laboratory of Brain Functional Genomics, East China Normal University, Shanghai, China
[b] Department of Neuroscience, Uppsala University, Uppsala, Sweden

ARTICLE INFO

Article history:
Received 9 January 2018
Received in revised form 14 August 2018
Accepted 11 September 2018
Available online 18 September 2018

Keywords:
miR-125b
NCAM
GSK3β
p-Tau
Presenilin-1/2
Dementia

ABSTRACT

MicroRNAs, small noncoding RNAs, not only regulate gene expression at the post-transcriptional level in a variety of physiological processes but also accompany the initiation and progression of a vast number of diseases, including dementia. While miR-125b has been shown to be aberrantly expressed in some dementia patients, its role in the pathological process remains ambiguous. Presenilin-1/2 conditional double knockout mice exhibit a range of symptoms, including impaired cognition and memory, increased tau phosphorylation, neuroinflammation, and apoptosis, and are therefore regarded as a useful dementia model. In the prefrontal cortices of double knockout mice, miR-125b was found to be abnormally increased in an age-dependent manner. We further verified the neural cell adhesion molecule (NCAM) as an miR-125b target using the dual luciferase reporter assay. The NCAM protein level was decreased when miR-125b was overexpressed (OE) in neuronal growth factor–induced differentiated PC12 cells, which further inhibited the neuronal growth factor–induced phosphorylation of glycogen synthase kinase 3 beta (GSK3β) at the Ser9 site and ultimately increased the GSK3β activity and tau phosphorylation. Moreover, on serum deprivation, high GSK3β activity in differentiated miR-125b-OE PC12 cells induced increased caspase-3 activation. Finally, adeno-associated virus–mediated miR-125b overexpression in the prefrontal cortexes of wild-type C57B/L6 mice resulted in decreased dendritic spine density. In addition, similar to the in vitro data, elevated GSK3β activity and hyperphosphorylation of the tau protein were confirmed. Taken together, our findings reveal a direct regulation of miR-125b on NCAM, which leads to further effects on downstream GSK3β activity and tau phosphorylation and may contribute to the generation of neurofibrillary tangles in neuropathological progression.

1. Introduction

Dementia is a major neurodegenerative disease that induces steady cognition and memory impairments, and symptoms of dementia aggravate gradually and eventually lead to death. Approximately 47.5 million patients worldwide suffer from some form of dementia (WHO, April 2016), including Alzheimer's disease (AD), vascular dementia, dementia with Lewy bodies, and frontotemporal dementia. Among the types of dementia, AD is one of the most common and previous studies have demonstrated dementia to be due to a consequence of multiple aberrant physiological progresses, for example, genetic mutations, aging, endocrine dysfunction and changes in biological signaling (Burns and Iliffe, 2009). Recently, some reports have highlighted the importance of microRNAs (miRNAs) in the progression of dementia and provided new insight into understanding the fundamental mechanism underlying this phenomenon (Ai et al., 2013; Lukiw, 2007; Lukiw et al., 2008; Sun et al., 2015).

miRNAs are small noncoding RNAs that can repress protein expression by post-transcriptionally binding to the 3′-untranslated regions (UTRs) of mRNAs (Abe and Bonini, 2013) and have emerged to play important roles in many physiological and pathophysiological processes, including neurodegenerative diseases (Bartel, 2004; Filipowicz et al., 2008). As a part of the RNase III family, Dicer is responsible for the maturation of miRNA (Lund and Dahlberg, 2006). Cerebral conditional Dicer knockout mice exhibited extensive miRNA deficiencies, which resulted in abnormal tau hyperphosphorylation (Hebert et al., 2010; Smith et al., 2011). Other studies showed that a variety of miRNAs,

* Corresponding author at: Key Laboratory of Brain Functional Genomics, MoE, East China Normal University, 3663 Zhongshan Road N., Shanghai 200062, China. Tel.: +86-21-62233970; fax: +86-21-62601953.
** Corresponding author at: Key Laboratory of Brain Functional Genomics, MoE, East China Normal University, 3663 Zhongshan Road N., Shanghai 200062, China. Tel.: +86-21-62232354; fax: +86-21-62601953.
E-mail addresses: bmei@brain.ecnu.edu.cn (B. Mei), bmeng@brain.ecnu.edu.cn (B. Meng).

0197-4580/$ – see front matter © 2018 Elsevier Inc. All rights reserved.
https://doi.org/10.1016/j.neurobiolaging.2018.09.011

including miR-9, miR-124, miR-132, and miR-137, could regulate splicing of the microtubule-associated protein tau. Moreover, tau-related protein kinases and phosphatases could be regulated by miR-15a, miR-16, miR-26a, miR-195, miR-497, etc (Hebert et al., 2010; Mohamed et al., 2010). Based on some clinical studies, pathological dementia processes are accompanied by changes in a variety of miRNAs, hinting that up- or downregulated miRNAs may take part in the nosogenesis or exacerbation of diseases (Alexandrov et al., 2012; Cogswell et al., 2008; Denk et al., 2015; Sethi and Lukiw, 2009; Wang et al., 2011). Previous studies have screened abnormal miRNAs in patients with AD, among which miR-125b was found to be upregulated in the medial frontal cortex, temporal lobe, hippocampus, cerebellum, and cerebrospinal fluid (Alexandrov et al., 2012; Cogswell et al., 2008; Sethi and Lukiw, 2009), and downregulated in serum (Galimberti et al., 2014; Jia and Liu, 2016; Kumar and Reddy, 2016; Tan et al., 2014). Thus, miR-125b has been reported as a promising biomarker for AD due to its correlation with the Mini Mental State Examination in patients with AD (Tan et al., 2014). In addition, studies using animal models have shown a correlation between miR-125b and pathological phenotypes, which enhances the importance of miR-125b in disease progression (Pogue et al., 2010; Yao et al., 2003).

Intriguingly, we found that presenilin-1/2 conditional double knockout (DKO) mice, which exhibited several early-onset preclinical phenotypes of dementia (progressive cognitive impairment [Saura et al., 2004; Wu et al., 2008], abnormal emotions [Yan et al., 2013], increased neuronal apoptosis [Saura et al., 2004], and hyperphosphorylation of tau protein [Feng et al., 2004]), could be used as an ideal dementia model. With its advantages, in this study, we performed a series of in vitro and in vivo analyses, to demonstrate that miR-125b can directly regulate the expression of neural cell adhesion molecule (NCAM), which is considered to play a crucial role in neuronal proliferation, survival, neurite outgrowth, etc (Ditlevsen et al., 2007; Jessen et al., 2001; Kolkova et al., 2000; Krushel et al., 1998; Liu et al., 2011; Schmid et al., 1999; Yang and Han, 2010). In addition, repression of NCAM by miR-125b affected glycogen synthase kinase 3 beta (GSK3β) activity and tau phosphorylation. Our findings suggest that the miR-125b regulation of NCAM may contribute to the formation of neurofibrillary tangles and be involved in of neuropathological progression.

2. Materials and methods

2.1. Mice

DKO mice were provided by Dr Tsien's laboratory (Feng et al., 2004). DKO (*Cre* +, *PS1* f/f, *PS2* −/−) and littermate (*Cre* −, *PS1* +/+, *PS2* +/+) mice were obtained by breeding heterozygous mice (*Cre* +, *PS1* f/+, *PS2* +/−), genotyping of offspring were carried out using standard PCR analysis. C57BL/6 mice were obtained from Shanghai SLAC Laboratory Animal Co Ltd, China. All the experiments were approved by the Institutional Animal Care and Use Committee of the East China Normal University (IACUC approval ID #M10020).

2.2. RNA isolation and quantitative real-time PCR

miRNAs and RNAs were isolated from prefrontal cortexes of DKO and littermate control mice using mirVana miRNA Isolation Kit (Ambion, AM1561). One microgram of total miRNAs was reverse-transcribed in a 20 μL reaction using miRcute miRNA First-Strand cDNA Synthesis kit (TIANGEN, KR211-01). Quantitation of miRNAs was carried out using miRcute miRNA qPCR Detection kit (TIANGEN, FP401). Ten nanogram cDNA was used as template in each reaction with specific primers to identify the certain miRNAs. Reverse primer was included in kit and sequences of forward primers are listed in Table 1. Quantitative real-time PCR was performed at 95 °C for 10 minutes, followed by 95 °C for 30 seconds, 60 °C for 30 seconds, and 72 °C for 30 seconds, 40 circles were applied. The amount of target genes was determined by the $2^{-\triangle\triangle Ct}$ and normalized to U6 as fold changes.

Table 1
Primer sequences of miRNAs

Primer name	Sequences (5′ to 3′)
GSP-miR-27b-3p	TTCACAGTGGCTAAGTTCTGC
GSP-miR-125b-5p	TCCCTGAGACCCTAACTTGTGA
GSP-miR-30e-5p	GAAGGTCAGTTCCTACAAATGT
GSP-miR-212-5p	TCATTCGTCAGATCTCGGTTCCA
GSP-miR-148b-3p	TGTTTCAAGACACTACGTGACT
GSP-miR-205-5p	GTCTGAGGCCACCTTACTTCCT
GSP-miR-141-3p	GGTAGAAATGGTCTGTCACAAT
GSP-miR-199a-5p	CTTGTCCATCAGACTTGTGACCC
GSP-miR-128-3p	TTTCTCTGGCCAAGTGACACT
U6-Forward	GCTTCGGCAGCACATATACTAAAAT
U6-Reverse	CGCTTCACGAATTTGCGTGTCAT

Key: miRNAs, microRNAs.

For mRNA quantifications, 2–5 μg mRNA was reverse-transcribed into cDNA using M-MLV reverse transcriptase (Invitrogen). Quantities of mRNA were measured by real-time PCR using SuperReal PreMix Plus (TIANGEN, FP205). Sequences of primers are shown in Table 2; glyceraldehyde-3-phosphate dehydrogenase (GAPDH) was used as the housekeeping gene and relative level of target genes was normalized against GAPDH.

2.3. Plasmid construction

NCAM-WT-F was a 26 bp sequence containing SEED that can be identified by miR-125b in NCAM 3′-UTR and NCAM-WT-R was the complementary sequence. NCAM-MUT-F had the same sequence as NCAM-WT-F except the changed SEED so that it could not be targeted by miR-125b. Xho I and Not I were added on both sides of each sequence. All sequences were synthesized by Invitrogen (NCAM-WT-F: TCGAGTGTGCTTCAGGGAAGTAGTGTCTCCTGC, NCAM-WT-R: GGCCGCAGGAGACACTACTTCCCTGAAGCACAC, NCAM-MUT-F: TCGAGTGTGCTGACTTTCAGTAGTGTCTCCTGC, NCAM-MUT-R: GGCCGCAGGAGACACTACTGAAAGTCAGCACAC). Complementary sequences were annealed and cloned into psiCHECK-2 vector (Promega) for constructs used in luciferase assay.

A 400 bp sequence that contains pri-miR-125b was amplified by PCR from mouse brain cDNA. Xho I and Kpn I sites were added on both sides of each sequence. PCR products were cloned into pEGFP-C1 vector for constructs used for in vitro transcription.

2.4. Cell culture, transfection, and treatments

A mouse neuroblastoma cell line, N2a, was maintained in DMEM medium plus 10% FBS, 1% penicillin, and 1% streptomycin; cells were

Table 2
Primer sequences of BDNF, ASIC1a, NCAM, and GAPDH

Primer name	Sequences (5′ to 3′)
BDNF-F	TCATACTTCGGTTGCATGAAGG
BDNF-R	AGACCTCTCGAACCTGCCC
ASIC1a-F	CACCTTCCCTGCCGTCACTC
ASIC1a-R	GCCCTGCTCTGTCGTAGAACTCA
NCAM-F	CACCTTCCCTGCCGTCACTC
NCAM-R	GCCCTGCTCTGTCGTAGAACTCA
GAPDH-F	ACCACAGTCCATGCCATCAC
GAPDH-R	TCCACCACCCTGTTGCTGTA

Key: BDNF, brain-derived neurotrophic factor; ASIC1a, acid-sensing ion channels 1a; GAPDH, glyceraldehyde-3-phosphate dehydrogenase; NCAM, neural cell adhesion molecule.

cultured in 5% CO_2 at 37 °C. miR-125b mimic/mimic controls (synthesized by Biotend Inc, Shanghai) and psiCHECK-NCAM-WT/MUT were diluted in Opti-MEMI, and co-transfection into N2a cells were performed with TurboFect (Fermentas) according to the instructions. Luciferase assays were performed 2 days after transfection with the Dual Luciferase assay System (Promega) with the guidance of the instruction.

PC12 cells were cultured in DMEM medium plus 10% HS, 5% FBS, 1% penicillin and 1% streptomycin. To establish stable transfected cells lines, pEGFP-miR-125/pEGFP-C1 were transfected to PC12 (named as PC12-125b-OE and PC12-con, respectively) similar to that in N2a, and then followed by G418 selection. The positive clones of G418-resistant transfected PC12 cells were further identified. For neuronal growth factor (NGF) treatment, cells were cultured in mediums that contained NGF (20 ng/mL) for 2 days before further analysis.

Apoptosis was induced by deprivation of serum. After NGF treatment, culture medium that contained NGF was replaced with fresh medium in which neither NGF nor serums was added.

2.5. Protein isolation and western blotting

For protein extraction, mice were anesthetized with chloral hydrate (300 mg/kg, i.p.). Prefrontal cortex was harvested on ice and then transferred to liquid nitrogen. Brain tissues were lysed with RIPA buffer added 1% PMSF, centrifuge at 1200 × g, supernatant fluid was collected and blending with loading buffer, then heated in water bath for 5 minutes. For protein obtained from cell lines, after removing culture medium and washing with HBSS, cells were harvested and added with loading buffer. Total protein were separated on 10% SDS-PAGE gel, transferred to 0.45 μm PVDF membrane and blocked with 5% BSA for 1 hour and then incubated with primary antibody overnight at 4 °C. The concentrations of primary antibodies were as follows: anti-NCAM, 1:1000 (Proteintech, 14255-1-AP); anti-GAPDH, 1:5000 (Proteintech, 60004-1-Ig); anti-GSK3β, 1:1000 (CST, 12456); anti-p-GSK3β-Ser9, 1:1000 (CST, 9323); anti-p-GSK3β-Tyr216, 1:1000 (BD, 612313); anti-p-tau-Ser396, 1:1000 (Life Technologies, 355300); anti-tau, (abcam, ab32057); anti-cleaved-caspase 3, 1:1000 (CST, 9664). After the overnight incubation, membranes were washed 3 times with TBST, and then incubated with HRP-conjugated second antibody (goat-anti-rabbit, 1:1000, biotime, A0208; goat-anti-mouse, 1:1000, biotime, A0216) for 2 hours at room temperature. Immunoreactivity was detected by enhanced chemiluminescence. Protein contents were analyzed with Quantity One. The amount of each protein was standardized as a ratio of protein to GAPDH. The ratios from all the groups were normalized by to control group and shown as a fold to the con during statistical analysis.

2.6. Stereotaxic injection

Adeno-associated virus (AAV) vectors were designed and constructed by Obio Technology (Shanghai) Corp., Ltd. Two-month-old C57BL/6 mice were used for injection. Mice were anesthetized with 10% (w/v) chloral hydrate and placed in a stereotactic frame. Microinjection needles were inserted (coordinates from Bregma: 1.7 AP, 0.2 ML, 1.8 DV) and virus suspensions were then injected at 100 nL per minute. After recovery, mice were housed at home cage with food and water provided *ad libitum*.

2.7. Golgi staining

Golgi staining was administered following manufacturer's instructions of FD Rapid GolgiStain Kit (FD Neuro Technologies). In brief, mice were anesthetized and brains were rapidly removed, transferred to premixed solution A and B, and then kept at temperature for 2 weeks. After being transferred and stored in solution C for 72 hours, coronal tissue sections of 120-μm thicknesses were sliced using freezing microtome (Leica). The dry slices were placed in a mixture consisting of solution D and E and double distilled water for 10 minutes. After gradient dehydration, slices were cleared in xylene and sealed with Permount. Dendritic spins were viewed with a light microscope (Leica). Spinal density of secondary apical dendrites was analyzed at proper segments (100 μm in length). As described by Nagy et al., 2011, the segments from a second-order dendrite protruding from their parent apical dendrite were chosen in each examined neuron for spine density quantification. Approximately 30 segments in each group were viewed and recorded for analysis. The ImageJ was used to measure the densities of spines. Image collection and data statistics were administered with double blind.

2.8. Statistical analysis

Data were analyzed by Student's *t*-test and presented as the mean ± SEM; Data of Quantitative real-time PCR and western blotting were normalized to control groups; $p < 0.05$ was considered as statistical significance.

3. Results

3.1. miR-125b was upregulated in the prefrontal cortex of DKO mice greater than 6 months old

Utilizing the benefits of early-onset dementia-like DKO mice, we analyzed the regulatory function of miR-125b in the neuropathological progression. We first measured the expression of miR-125b in the prefrontal cortexes (PFCs) of 2-, 6-, and 12-month-old DKO mice as well as in their littermate controls. Notably, miR-125b was significantly increased in the PFCs of 6- and 12-month-old DKO mice compared with that in their wild-type littermates (Fig. 1).

3.2. miR-125b is a potential regulator of NCAM-140/180, but not NCAM-120, in DKO mouse brains

To identify the importance of miR-125b in the progression of dementia in DKO mice, TargetScan (bioinformatics software) was performed to predict potential miR-125b targets. Of more than 3000 predicted target genes, brain-derived neurotrophic factor (BDNF), acid-sensing ion channels 1a (ASIC1a), and neural cell adhesion molecule (NCAM) were selected and further evaluated due to their important roles in neurogenesis, neuron survival and connection, cognition, learning, and memory (Bisaz et al., 2013; Ditlevsen et al., 2007; Huang and Reichardt, 2001; Wemmie et al., 2002; Wu et al., 2016; Yew et al., 1999). Based on the post-translational manipulating property of miRNAs, we measured the mRNA expression of BDNF, ASIC1a, and NCAM in the PFCs of 12-month-old DKO mice. The relative transcription of NCAM, but not of BDNF or ASIC, was notably decreased in the PFCs of DKO mice (Fig. 2A). In addition, an age-dependent reduction in NCAM mRNA expression was observed in the PFCs of DKO mice (Fig. 2B), suggesting a potential regulation between miR-125b and NCAM.

To exclude the possibility that NCAM is regulated by other miRNAs, we further tested multiple miRNAs that were predicted to target the NCAM 3′-UTR, including miR-30e-5p, miR-128-3p, miR-148-3p, miR-27-3p, miR-141-3p, miR-199a-5p, miR-125b-5p, miR-212-5p, and miR-205-5p. Real-time quantitative PCR was used to detect miRNA levels in the PFCs of DKO mice and their littermate controls. Compared with the controls, a significant increase in miR-125b expression (Supplementary Figure S1), but not in the

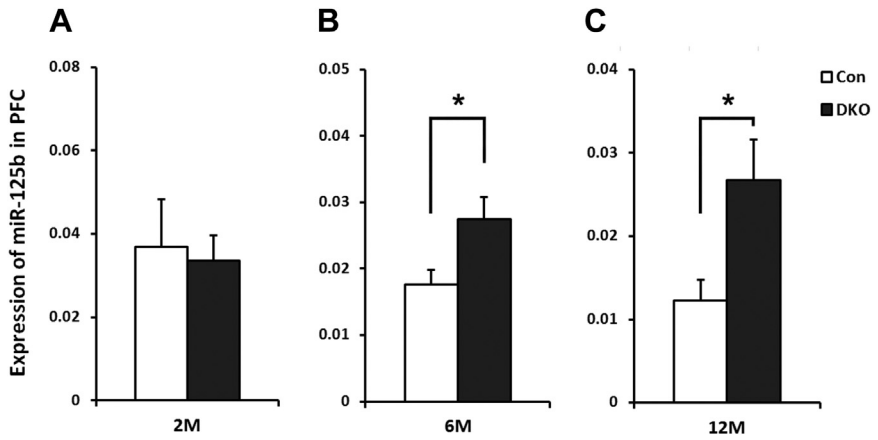

Fig. 1. miR-125b expression was increased in the PFC of 6- and 12-month-old, but not 2-month-old DKO mice. The expression levels of miR-125b in the PFCs of (A) 2-, (B) 6-, and (C) 12-month-old DKO and control mice were measured with quantitative real-time PCR (n = 3 biological replicates for each group; data was shown as mean ± SEM, Student's *t*-test, $^{*}p < 0.05$). Abbreviations: DKO, double knockout; PFCs, prefrontal cortexes.

expression of the other miRNAs listed previously, was observed in the PFCs of the 12-month-old DKO mice. These results indicated a high correlation between miR-125b and NCAM in the PFCs of DKO mice.

In addition, NCAM has 3 isoforms that are named according to their molecular sizes determined by alternative splicing (Barbas et al., 1988). Blasting the UTR sequences of NCAM-120, NCAM-140 and NCAM-180 revealed that those of NCAM-140 and NCAM-180 were identical, and thus further evaluated these 2 NCAM protein isoforms. Compared with their littermates, NCAM-140 and NCAM-180 were expressed at significantly lower levels in the PFCs of 12-month-old DKO mice. However, no difference was observed in NCAM-120 content between the DKO and their littermate controls (Fig. 2C).

3.3. NCAM-140/180 expression was regulated by miR-125b in vitro

To further investigate the relationship between miR-125b and NCAM, we used a dual luciferase report assay system to detect the inhibition of miR-125b on NCAM 3′-UTR "SEED sequence". The "SEED sequence" was cloned downstream of the synthetic Renilla luciferase gene in the psiCHECK-2 vector (Fig. 3A), and miR-125b

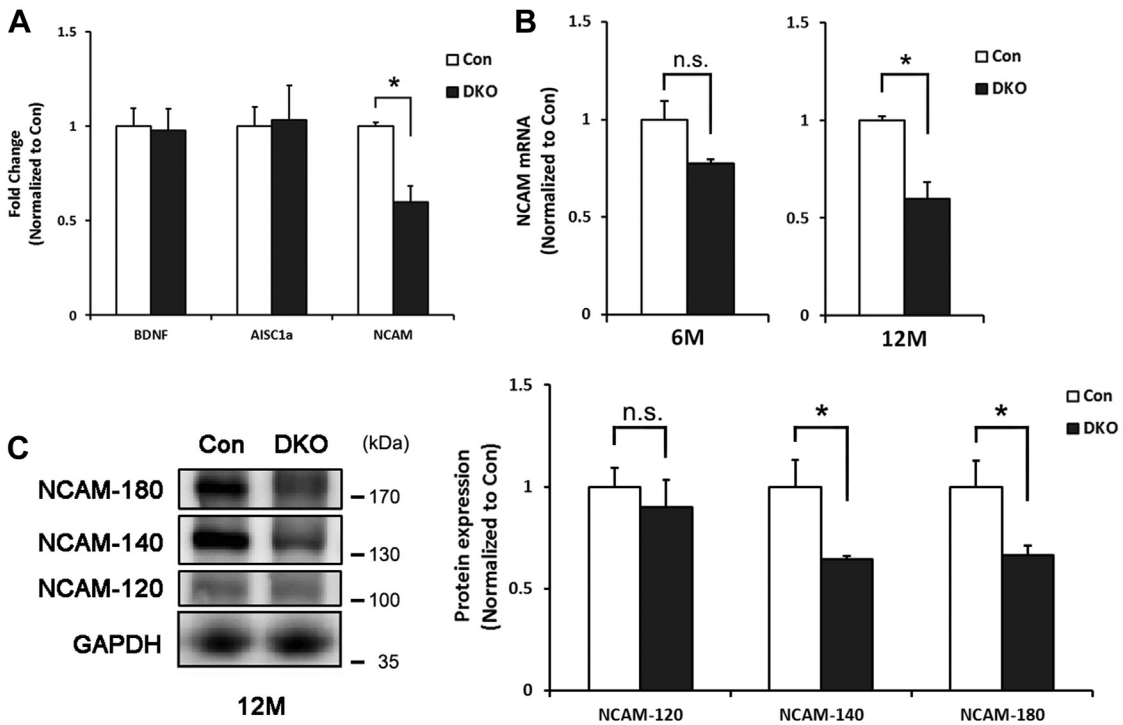

Fig. 2. Predicted target NCAM expression in the PFCs of DKO mice. (A) Relative mRNA levels of 3 predicted miR-125b targets, BDNF, ASIC1a and NCAM, in the PFCs of 12-month-old DKO mice, compared with those in control mice. (B) NCAM mRNA expression was significantly reduced in the PFCs of 12-month-old DKO mice. (C) Western blot analysis showing that the protein expression levels of NCAM-140 and NCAM-180, but not of NCAM-120, were decreased in the PFCs of 12-month-old DKO mice. (n = 3 biological replicates for each group; the data was normalized to the control group and shown as mean ± SEM, Student's *t*-test, $^{*}p < 0.05$). Abbreviations: BDNF, brain-derived neurotrophic factor; ASIC1a, acid-sensing ion channels 1a; DKO, double knockout; PFCs, prefrontal cortexes; NCAM, neural cell adhesion molecule; n.s., not significant.

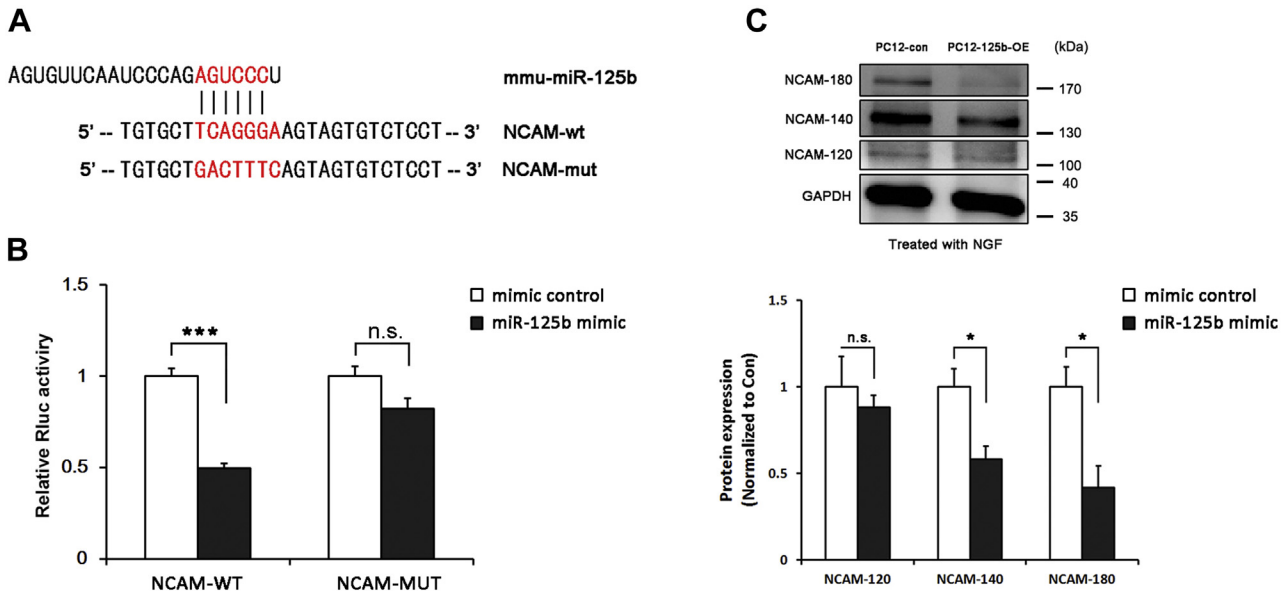

Fig. 3. miR-125b regulated NCAM translation in vitro. (A) A sequence (NCAM-WT) containing the site of miR-125b regulation (red bases) as well as a control sequence (NCAM-MUT) containing the mutant bases were cloned from the NCAM 3′-UTR. (B) Dual luciferase assay results showing that the miR-125b mimics decreased the luciferases activity in N2a cells transfected with the dual luciferase reporter plasmid containing the NCAM 3-UTR. (C) Western blot showed that with NGF treatment, NCAM-140 and NCAM-180, but not NCAM-120, were suppressed in miR-125b-overexpressing PC12 cells (PC12-125b-OE, PC12 cells overexpressing miR-125b; PC12-con, control PC12 cells). (n = 3 biological replicates for each group; the data was normalized to the control group and shown as mean ± SEM, Student's *t*-test, $^{*}p < 0.05$, $^{***}p < 0.001$). Abbreviations: NCAM, neural cell adhesion molecule; n.s., not significant; NGF, neuronal growth factor; UTR, untranslated region. (For interpretation of the references to color in this figure legend, the reader is referred to the Web version of this article.)

mimics with recombinant plasmids were then co-transfected into N2a cells. The ratio of the Renilla luminescence signal to the firefly signal reflected the inhibitory effects of the miRNA mimics to the sequences cloned into the psiCHECK-2 vector. Co-transfection of the miR-125b mimics and psiCHECK-NCAM-UTR (NCAM-WT) revealed significantly lower Renilla luciferase activity compared with that in the other groups (Fig. 3B), suggesting that miR-125b suppresses the expression of Renilla luciferase by targeting NCAM 3′-UTR sequences.

The suppression of miR-125b was further confirmed in neurogenic PC12 cells. PC12 cells can be differentiated into sympathetic neuron-like cells with the administration of NGF. *Howard* et al. observed that the differentiation of PC12 cells NGF was accompanied by increased NCAM expression (Prentice et al., 1987). Thus we established a PC12 cell line overexpressing miR-125b (PC12-125b-OE) and its control line (PC12-con) (Supplementary Figure S2). After NGF treatment for 48 hours, the expression levels of NCAM-140 and NCAM-180, but not of NCAM-120, were significantly lower in PC12-125b-OE cells than those in PC12-con cells (Fig. 3C). Therefore, we assumed that miR-125b can directly target the 3′-UTRs of NCAM-140/180 and suppress their translation.

3.4. The regulation of miR-125b on NCAM-140/180 affected the GSK3β activity and tau phosphorylation in PC12 cells

A previous study verified that the neuroprotective effect of NCAM relies on enhancing the phosphorylation of GSK3β at the inhibitory Ser9 site (Klementiev et al., 2007). Thus, we measured the activity of GSK3β, which can be reflected by the p-GSK3β-Tyr216 level and the ratio of p-GSK3β-Ser9 to GSK3β, in PC12-125b-OE and control cells with or without NGF treatment. No differences in GSK3β expression or GSK3β phosphorylation were observed before NGF treatment (Supplementary Figure S3). After treatment with NGF, obviously decreased phosphorylated Ser9-GSK3β levels were detected in PC12-125b-OE cells compared with that in control cells (Fig. 4A). However, miR-125b had no effect on pGSK3β-Tyr216 (Fig. 4A). Because GSK3β is a key protein kinase in phosphorylation of tau protein, we next examined the phosphorylation of this protein in PC12-125b-OE cells. No significant expression change of total tau was observed in miR-125b overexpressed PC12 cells (see Supplementary Figure S4), similar with the unchanged total tau expression in DKO mice (Supplementary Figure S5). While on NGF treatment, there was a remarkable increase of tau phosphorylated at Ser-396 site (Fig. 4B), consistent with the elevated activity of GSK3β in PC12-125b-OE cells compared with control cells.

Because nutrient deficiency-induced cellular apoptosis is accompanied by increased GSK3β activity (Bhat et al., 2000, 2002), we wondered whether the neuronal losses in DKO mice were associated with miR-125b upregulation and GSK3β hyperactivation. Thus, we further evaluated whether the increased activity of GSK3β in PC12-125b-OE cells could affect apoptosis after nutrient withdrawal. After 3 hours of serum deprivation, elevated GSK3β phosphorylation at the Tyr216 site (Fig. 4C) and reduced GSK3β phosphorylation at the Ser9 site were detected in PC12-125b-OE cells (Fig. 4C). Consistently, cleaved caspase-3 levels in PC12-125b-OE were remarkably elevated compared with those in PC12-con cells (Fig. 4D), an association between NCAM and GSK3β was clearly established (Corbett et al., 2013; Klementiev et al., 2007; Liu et al., 2011). Phosphorylation of the tau protein was also obviously increased in PC12-125b-OE cells (Fig. 4E). Therefore, we concluded that the effect of miR-125b upregulation was most likely mediated by NCAM reduction.

3.5. Overexpression of miR-125b in the PFCs increased GSK3β activity and tau protein phosphorylation in mice

To verify the effects of miR-125b regulation on GSK3β and tau protein phosphorylation in vivo, we bilaterally injected AAV-miR-125b into the PFCs of 2-month-old C57BL/6 mice (Fig. 5A), which

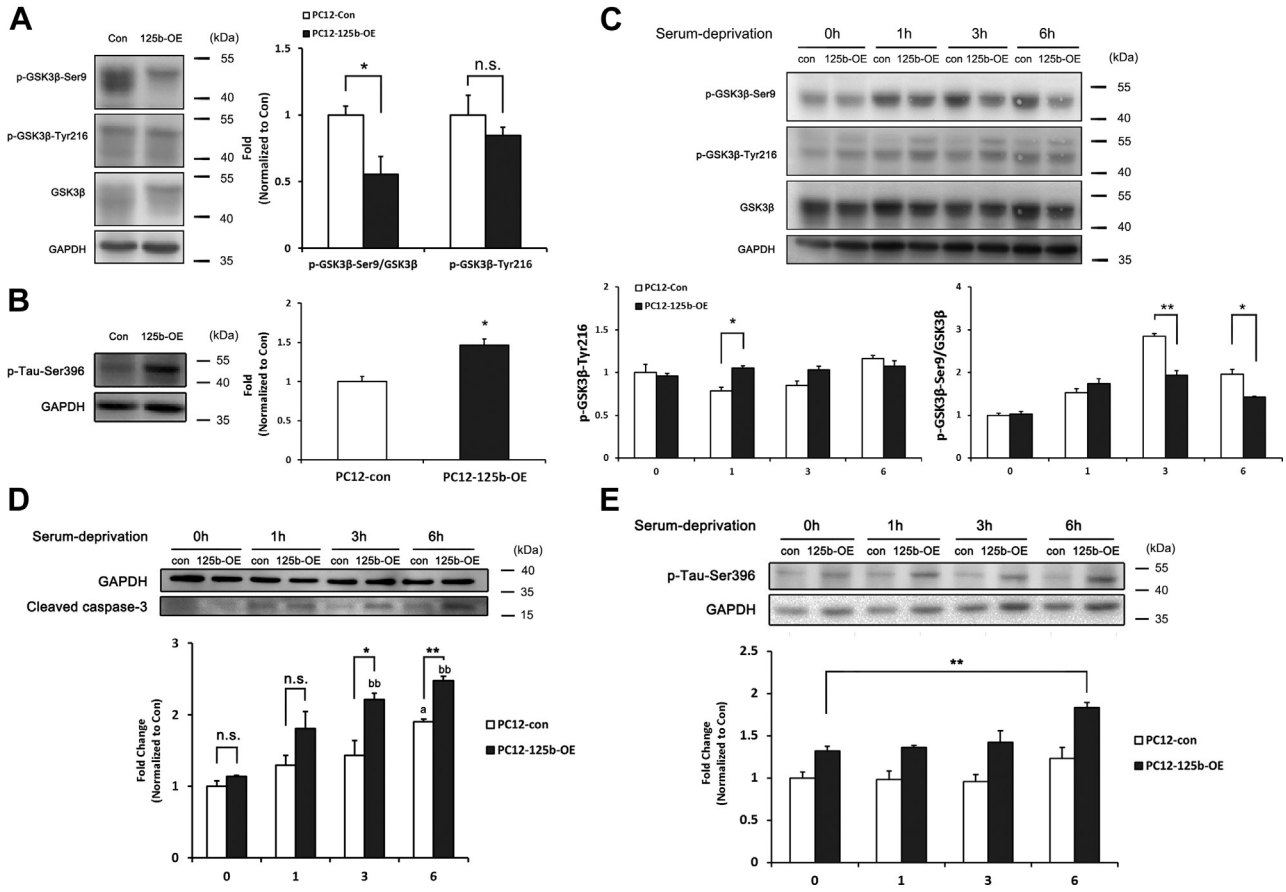

Fig. 4. miR-125b promoted GSK3β activity, tau phosphorylation, and apoptosis in vitro. (A) After 48 hours of NGF treatment, the ratio of phosphorylated GSK3β at the Ser9 site to total GSK3β, but not phosphorylated GSK3β at the Tyr216 site, was reduced in PC12-125b-OE cells. (B) Expression of the phosphorylated tau protein was increased in PC12-125b-OE cells with NGF induction. (C) Increased GSK3β activity was detected after serum deprivation. (D) The caspase-3 activity in PC12-125b-OE cells was significantly increased. (E) Tau phosphorylation was obviously increased in PC12-125b-OE cells. (n = 3 biological replicates for each group; the data were normalized to the control group and shown as mean ± SEM, Student's *t*-test, $^{*}p < 0.05$, $^{**}p < 0.01$, $^{a}p < 0.05$, compared with 0 group of PC12-con; $^{bb}p < 0.01$, compared with 0 group of PC12-125b-OE). Abbreviations: GSK3β, glycogen synthase kinase 3 beta; NGF, neuronal growth factor; n.s., not significant.

increased miR-125b expression approximately 4-fold. Four months after the AAV infection, increased phosphorylation of GSK3β at the Tyr216 site was observed in AAV-miR-125b–infected tissues, whereas the ratio of p-GSK3β-Ser9 to total GSK3β was not significantly altered (Fig. 5B). Furthermore, phosphorylation of the tau protein was remarkably increased in PFCs overexpressing miR-125b (Fig. 5C). In addition, obvious hyperphosphorylation of the tau protein was observed in the PFCs of 12-month-old DKO mice (Fig. 5C). Our results revealed that the regulation of miR-125b on NCAM could effectively increase GSK3β activity and tau phosphorylation in vivo, which might contribute to the formation of neurofibrillary tangles.

As another hallmark of dementia, decreased dendritic spines density is a universal clinical symptom. Owing to the functions of NCAM in cell-cell adhesions and interactions, we tested the spine densities in C57BL/6 mice that had been overexpressing miR-125b for 4 months. Using Golgi staining, we found that the spine densities in miR-125b-overexpressing PFCs were less than those in the controls (Fig. 5D), which revealed the importance of miR-125b in physiological procedures. Taken together, our results validated a direct relationship between miR-125b and NCAM. Downregulation of NCAM-140/180 most likely affects GSK3β activation and induces progressive neural dysfunction. In addition, the NCAM reduction might be associated with the loss of dendritic spines. These data may provide a new insight into the causation of dementia and help identify potential clinical therapeutic targets.

4. Discussion

Dementia has become one of the most public health hazards, and although studies on dementia have been a hot topic since the 19th century, the fundamental mechanisms underlying this disease are still not fully elucidated. The causes of dementia are controversial and undefined, for example, AD may be caused by genetic mutants, amyloid-beta toxicity, tauopathy, cholinergic system dysfunction, vascular injury, etc (Barger and Harmon, 1997; Lesne et al., 2006; Mortimer et al., 2004; Watanabe et al., 2009). One of the potential pathogenic risks of dementia is the misregulation of miRNAs.

Upregulation of miR-125b has been highlighted in studies on AD patients and animal models, and is proposed to be involved in driving pathogenic signaling (Cheng et al., 2013; Lukiw, 2007). In DKO mice, miR-125b expression was significantly increased in an age-dependent manner. Despite the fact that the mechanism underlying miR-125b remains unclear, its role in dementia progression has been highlighted (Alexandrov et al., 2012; Cogswell et al., 2008; Kumar and Reddy, 2016; Sethi and Lukiw, 2009; Tan et al., 2014). We showed that a predicted target of miR-125b, NCAM, was remarkably decreased transcriptionally, and its mRNA expression was negatively correlated with the miR-125b expression level. In the central nervous system, NCAM participates in a variety of cellular processes including neurite outgrowth and extension (Jessen et al., 2001; Kolkova et al., 2000; Schmid et al., 1999), neuronal survival (Ditlevsen et al., 2007), and proliferation (Krushel

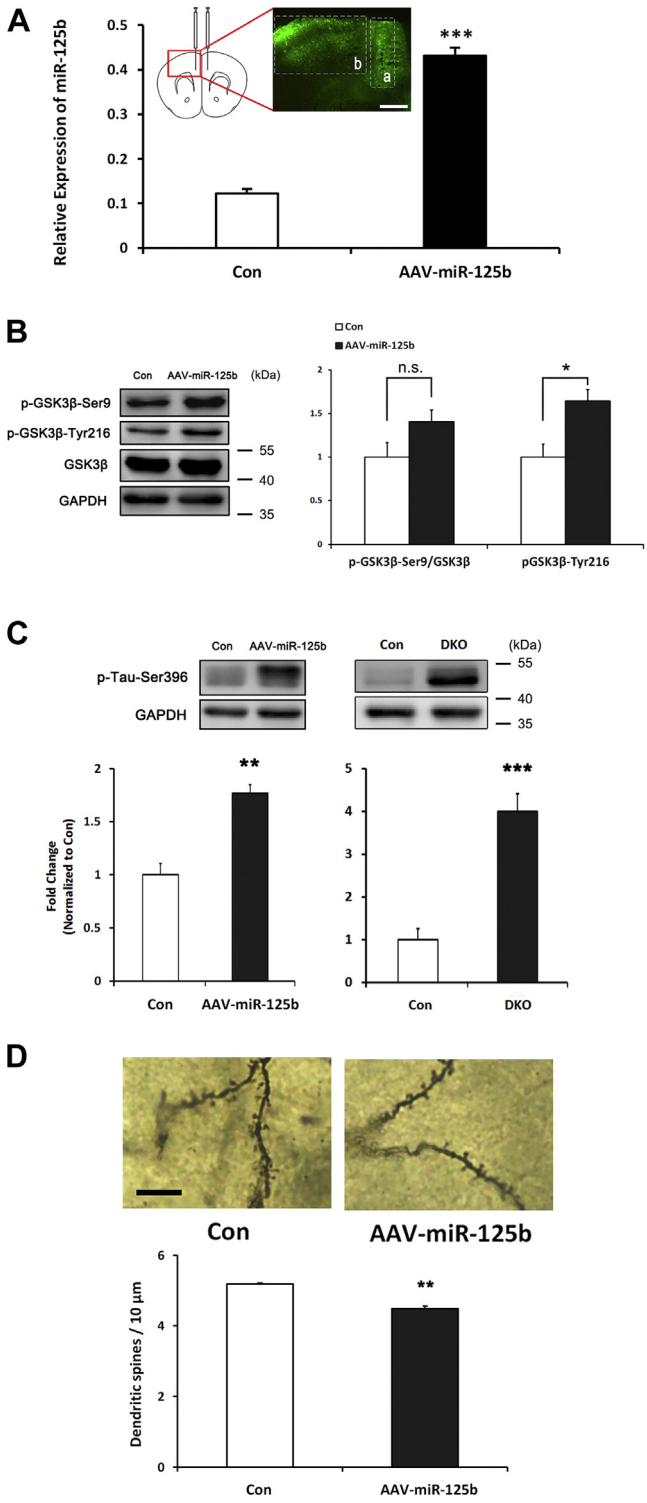

Fig. 5. Overexpression of miR-125b in the PFCs induced GSK3β hyperactivity, tau phosphorylation, and dendritic spine density reduction. (A) Quantitative RT-PCR analysis showing that the stereotaxic injection of adeno-associated virus (AAV)-miR-125b significantly increased of miR-125b expression in the PFCs of 2-month-old C57BL/6 mice. The dotted box (a) indicates the injection position, whereas the dotted box (b) indicates the infected region. Scale bar, 500 μm. (B) Western blot analysis showing that the expression levels of p-GSK3β-Ser9 and p-GSK3β-Tyr216 were upregulated in PFCs infected with AAV for 4 months (AAV-miR-125b and con), while total GSK3β and the p-GSK3β-Ser9/GSK3β ratio were not altered. (C) Phosphorylation of tau protein in the PFCs of AAV-miR-125b–infected mouse brains was significantly increased, similar to that in DKO mice. (D) Golgi staining showing lower spine densities in AAV-miR-125b–infected mice; scale bar, 10 μm. (n = 3 biological replicates for each group; the data were normalized to the control group and shown as mean ± SEM, Student's *t*-test, $^{*}p < 0.05$, $^{**}p < 0.01$, $^{***}p < 0.001$). Abbreviations: DKO, double knockout; GSK3β, glycogen synthase kinase 3 beta; PFCs, prefrontal cortexes; n.s., not significant.

et al., 1998; Liu et al., 2011; Yang and Han, 2010). More importantly, NCAM is involved in the development and plasticity of the nervous system, which contributes to the formation and consolidation of memory (Ronn et al., 1998; Rose, 1996). Most dementia syndromes including AD, vascular dementia, and frontotemporal dementia, are characterized by the progressive loss of neurons, decreased neuronal plasticity, and synaptogenesis disturbance. The reduction of NCAM in the cortex was shown to contribute to the initiation of synapse loss in AD (Aisa et al., 2010; Leshchyns'ka et al., 2015). Despite the critical role of NCAM, epigenetic regulation of NCAM in the dementia process has rarely been investigated. Herein, we demonstrated that miR-125b directly inhibited NCAM-140/180 translation, which potentially contributes to the decreased NCAM protein expression in cortices of patients with AD. Morphologically, dendritic spines participate in neuronal connections, which are required for the maintenance of brain function. In addition, we also observed that overexpressing miR-125b in the PFCs of C57BL/6 mice led to defective recognition and memory abilities in a novel object recognition task (unpublished data). Although more rigorous stereological methods should be used for dendritic spine quantification in the future, which is an inadequacy in our analysis, the reduced densities of dendritic spines in mice overexpressing miR-125b in their PFCs and in DKO mice were obvious, and given the important role of NCAM in spine dynamics and synaptogenesis (Muller et al., 2010), the reduced densities of dendritic spines in mice overexpressing miR-125b in their PFCs and in DKO mice might result from the downregulation of NCAM expression.

In addition, the neuroprotective role of NCAM relies on the fibroblast growth factor receptor, which leads to GSK3β phosphorylation at the Ser9 site (Klementiev et al., 2007). GSK3β, which is highly activated in patients with AD (Ferrer et al., 2002, 2005; Leroy et al., 2007), has been comprehensively investigated. The tau protein binds microtubules and maintains axon structures and neuronal outgrowth under normal physiological conditions (Ramsden et al., 2005; Weingarten et al., 1975). Based on the regulatory effect of NCAM on GSK3β, we further evaluated the activity of GSK3β by overexpressing miR-125b both in vitro and in vivo. In accordance with our expectation, GSK3β phosphorylation at the Ser9 site was reduced in PC12 cells, which may have resulted in the disinhibition of GSK3β activity. In C57BL/6 mice, an elevation in GSK3β phosphorylation at the Tyr216 site was detected, which could also cause GSK3β activation. This subtle inconstancy might be due to the complexity of the in vivo environment. However, in cell cultures, the effect of miR-125b was possibly via direct and straightforward regulation, as GSK3β hyperactivation led to increased tau phosphorylation, which was also detected in the PFCs of 12-month-old DKO mice.

PS1 and PS2, the components of γ-secretase, have been shown to participate in the production of Aβ and to be closely related to the pathology of familial AD (Haass, 1997; Sherrington et al., 1995). Interestingly, no excessive Aβ deposition due to dysfunctional γ-secretase resulting from the conditional forebrain knockout of PS1 and PS2 was observed in DKO mice. These nonamyloidgenic dementia-like symptoms suggested that the occurrence and development of dementia might be associated with other factors such as tauopathy. Moreover, clinical studies have indicated that the GSK3β activity was elevated in the brains of AD patients, highlighting the involvement of tau hyper-phosphorylation in neurodegenerative procedures (Ferrer et al., 2002, 2005; Leroy et al., 2007). Thus, we suggest that further attention should be paid to the importance of the miR-125b-NCAM-GSK3β interaction.

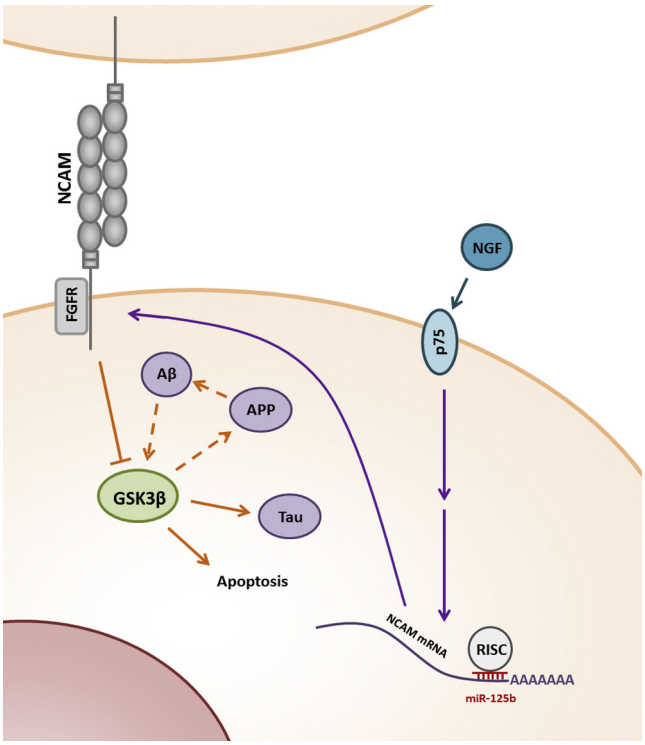

Fig. 6. Schematic illustration of miR-125b regulation to NCAM and effect to downstream signals (see text for details). Abbreviation: NCAM, neural cell adhesion molecule.

5. Conclusions

In summary, our study first validated the regulation of miR-125b on NCAM, which influences the stabilization of spine dynamics. The repression of aberrant miR-125b upregulation promotes tau phosphorylation by activating GSK3β (Fig. 6). Our findings emphasize the contribution of miR-125b to the pathological process of dementia including the formation of neurofibrillary tangles. However, more verifications and analyses, including whether the early interference of abnormally increased miR-125b expression may rescue, or at least attenuate NCAM cleavage, and tau hyperphosphorylation in dementia are indispensable.

Disclosure statement

The authors declare no actual or potential conflicts of interest.

Acknowledgements

This work was supported by the National Natural Science Foundation of China, China (31271133, 31100748, 31771116), and Natural Science Foundation of Shanghai, China (17ZR1408100).

Appendix A. Supplementary data

Supplementary data to this article can be found online at https://doi.org/10.1016/j.neurobiolaging.2018.09.011.

References

Abe, M., Bonini, N.M., 2013. MicroRNAs and neurodegeneration: role and impact. Trends Cell Biol. 23, 30–36.
Ai, J., Sun, L.H., Che, H., Zhang, R., Zhang, T.Z., Wu, W.C., Su, X.L., Chen, X., Yang, G., Li, K., Wang, N., Ban, T., Bao, Y.N., Guo, F., Niu, H.F., Zhu, Y.L., Zhu, X.Y., Zhao, S.G., Yang, B.F., 2013. MicroRNA-195 protects against dementia induced by chronic brain hypoperfusion via its anti-amyloidogenic effect in rats. J. Neurosci. 33, 3989–4001.
Aisa, B., Gil-Bea, F.J., Solas, M., Garcia-Alloza, M., Chen, C.P., Lai, M.K., Francis, P.T., Ramirez, M.J., 2010. Altered NCAM expression associated with the cholinergic system in Alzheimer's disease. J. Alzheimers Dis. 20, 659–668.
Alexandrov, P.N., Dua, P., Hill, J.M., Bhattacharjee, S., Zhao, Y., Lukiw, W.J., 2012. microRNA (miRNA) speciation in Alzheimer's disease (AD) cerebrospinal fluid (CSF) and extracellular fluid (ECF). Int. J. Biochem. Mol. Biol. 3, 365–373.
Barbas, J.A., Chaix, J.C., Steinmetz, M., Goridis, C., 1988. Differential splicing and alternative polyadenylation generates distinct NCAM transcripts and proteins in the mouse. EMBO J. 7, 625–632.
Barger, S.W., Harmon, A.D., 1997. Microglial activation by Alzheimer amyloid precursor protein and modulation by apolipoprotein E. Nature 388, 878–881.
Bartel, D.P., 2004. MicroRNAs: genomics, biogenesis, mechanism, and function. Cell 116, 281–297.
Bhat, R.V., Leonov, S., Luthman, J., Scott, C.W., Lee, C.M., 2000. Regulation and localization of tyrosine216 phosphorylation of glycogen synthase kinase-3beta in cellular and animal models of neuronal degeneration. Proc. Natl. Acad. Sci. U. S. A. 97, 11074–11079.
Bhat, R.V., Shanley, J., Correll, M.P., Fieles, W.E., Keith, R.A., Scott, C.W., Lee, C.M., 2002. Interactions between GSK3beta and caspase signalling pathways during NGF deprivation induced cell death. J. Alzheimers Dis. 4, 291–301.
Bisaz, R., Boadas-Vaello, P., Genoux, D., Sandi, C., 2013. Age-related cognitive impairments in mice with a conditional ablation of the neural cell adhesion molecule. Learn. Mem. 20, 183–193.
Burns, A., Iliffe, S., 2009. Dementia. BMJ 338, b75.
Cheng, X.R., Cui, X.L., Zheng, Y., Zhang, G.R., Li, P., Huang, H., Zhao, Y.Y., Bo, X.C., Wang, S.Q., Zhou, W.X., Zhang, Y.X., 2013. Nodes and biological processes identified on the basis of network analysis in the brain of the senescence accelerated mice as an Alzheimer's disease animal model. Front. Aging Neurosci. 5, 65.
Cogswell, J.P., Ward, J., Taylor, I.A., Waters, M., Shi, Y., Cannon, B., Kelnar, K., Kemppainen, J., Brown, D., Chen, C., Prinjha, R.K., Richardson, J.C., Saunders, A.M., Roses, A.D., Richards, C.A., 2008. Identification of miRNA changes in Alzheimer's disease brain and CSF yields putative biomarkers and insights into disease pathways. J. Alzheimers Dis. 14, 27–41.
Corbett, N.J., Gabbott, P.L., Klementiev, B., Davies, H.A., Colyer, F.M., Novikova, T., Stewart, M.G., 2013. Amyloid-beta induced CA1 pyramidal cell loss in young adult rats is alleviated by systemic treatment with FGL, a neural cell adhesion molecule-derived mimetic peptide. PLoS One 8, e71479.
Denk, J., Boelmans, K., Siegismund, C., Lassner, D., Arlt, S., Jahn, H., 2015. MicroRNA Profiling of CSF reveals potential biomarkers to detect Alzheimer`s disease. PLoS One 10, e0126423.
Ditlevsen, D.K., Berezin, V., Bock, E., 2007. Signalling pathways underlying neural cell adhesion molecule-mediated survival of dopaminergic neurons. Eur. J. Neurosci. 25, 1678–1684.
Feng, R., Wang, H., Wang, J., Shrom, D., Zeng, X., Tsien, J.Z., 2004. Forebrain degeneration and ventricle enlargement caused by double knockout of Alzheimer's presenilin-1 and presenilin-2. Proc. Natl. Acad. Sci. U. S. A. 101, 8162–8167.
Ferrer, I., Barrachina, M., Puig, B., 2002. Glycogen synthase kinase-3 is associated with neuronal and glial hyperphosphorylated tau deposits in Alzheimer's disease, Pick's disease, progressive supranuclear palsy and corticobasal degeneration. Acta Neuropathol. 104, 583–591.
Ferrer, I., Gomez-Isla, T., Puig, B., Freixes, M., Ribe, E., Dalfo, E., Avila, J., 2005. Current advances on different kinases involved in tau phosphorylation, and implications in Alzheimer's disease and tauopathies. Curr. Alzheimer Res. 2, 3–18.
Filipowicz, W., Bhattacharyya, S.N., Sonenberg, N., 2008. Mechanisms of post-transcriptional regulation by microRNAs: are the answers in sight? Nat. Rev. Genet. 9, 102–114.
Galimberti, D., Villa, C., Fenoglio, C., Serpente, M., Ghezzi, L., Cioffi, S.M., Arighi, A., Fumagalli, G., Scarpini, E., 2014. Circulating miRNAs as potential biomarkers in Alzheimer's disease. J. Alzheimers Dis. 42, 1261–1267.
Haass, C., 1997. Presenilins: genes for life and death. Neuron 18, 687–690.
Hebert, S.S., Papadopoulou, A.S., Smith, P., Galas, M.C., Planel, E., Silahtaroglu, A.N., Sergeant, N., Buee, L., De Strooper, B., 2010. Genetic ablation of Dicer in adult forebrain neurons results in abnormal tau hyperphosphorylation and neurodegeneration. Hum. Mol. Genet. 19, 3959–3969.
Huang, E.J., Reichardt, L.F., 2001. Neurotrophins: roles in neuronal development and function. Annu. Rev. Neurosci. 24, 677–736.
Jessen, U., Novitskaya, V., Pedersen, N., Serup, P., Berezin, V., Bock, E., 2001. The transcription factors CREB and c-Fos play key roles in NCAM-mediated neuritogenesis in PC12-E2 cells. J. Neurochem. 79, 1149–1160.
Jia, L.H., Liu, Y.N., 2016. Downregulated serum miR-223 servers as biomarker in Alzheimer's disease. Cell Biochem. Funct. 34, 233–237.
Klementiev, B., Novikova, T., Novitskaya, V., Walmod, P.S., Dmytriyeva, O., Pakkenberg, B., Berezin, V., Bock, E., 2007. A neural cell adhesion molecule-derived peptide reduces neuropathological signs and cognitive impairment induced by Abeta25-35. Neuroscience 145, 209–224.
Kolkova, K., Novitskaya, V., Pedersen, N., Berezin, V., Bock, E., 2000. Neural cell adhesion molecule-stimulated neurite outgrowth depends on activation of protein kinase C and the Ras-mitogen-activated protein kinase pathway. J. Neurosci. 20, 2238–2246.
Krushel, L.A., Tai, M.H., Cunningham, B.A., Edelman, G.M., Crossin, K.L., 1998. Neural cell adhesion molecule (N-CAM) domains and intracellular signaling pathways

involved in the inhibition of astrocyte proliferation. Proc. Natl. Acad. Sci. U. S. A. 95, 2592–2596.
Kumar, S., Reddy, P.H., 2016. Are circulating microRNAs peripheral biomarkers for Alzheimer's disease? Biochim. Biophys. Acta 1862, 1617–1627.
Leroy, K., Yilmaz, Z., Brion, J.P., 2007. Increased level of active GSK-3beta in Alzheimer's disease and accumulation in argyrophilic grains and in neurones at different stages of neurofibrillary degeneration. Neuropathol. Appl. Neurobiol. 33, 43–55.
Leshchyns'ka, I., Liew, H.T., Shepherd, C., Halliday, G.M., Stevens, C.H., Ke, Y.D., Ittner, L.M., Sytnyk, V., 2015. Abeta-dependent reduction of NCAM2-mediated synaptic adhesion contributes to synapse loss in Alzheimer's disease. Nat. Commun. 6, 8836.
Lesne, S., Koh, M.T., Kotilinek, L., Kayed, R., Glabe, C.G., Yang, A., Gallagher, M., Ashe, K.H., 2006. A specific amyloid-beta protein assembly in the brain impairs memory. Nature 440, 352–357.
Liu, R., Shi, Y., Yang, H.J., Wang, L., Zhang, S., Xia, Y.Y., Wong, J.L., Feng, Z.W., 2011. Neural cell adhesion molecule potentiates the growth of murine melanoma via beta-catenin signaling by association with fibroblast growth factor receptor and glycogen synthase kinase-3beta. J. Biol. Chem. 286, 26127–26137.
Lukiw, W.J., 2007. Micro-RNA speciation in fetal, adult and Alzheimer's disease hippocampus. Neuroreport 18, 297–300.
Lukiw, W.J., Zhao, Y., Cui, J.G., 2008. An NF-kappaB-sensitive micro RNA-146a-mediated inflammatory circuit in Alzheimer disease and in stressed human brain cells. J. Biol. Chem. 283, 31315–31322.
Lund, E., Dahlberg, J.E., 2006. Substrate selectivity of exportin 5 and Dicer in the biogenesis of microRNAs. Cold Spring Harb. Symp. Quant. Biol. 71, 59–66.
Mohamed, J.S., Lopez, M.A., Boriek, A.M., 2010. Mechanical stretch up-regulates microRNA-26a and induces human airway smooth muscle hypertrophy by suppressing glycogen synthase kinase-3beta. J. Biol. Chem. 285, 29336–29347.
Mortimer, J.A., Gosche, K.M., Riley, K.P., Markesbery, W.R., Snowdon, D.A., 2004. Delayed recall, hippocampal volume and Alzheimer neuropathology: findings from the Nun Study. Neurology 62, 428–432.
Muller, D., Mendez, P., Deroo, M., Klauser, P., Steen, S., Poglia, L., 2010. Role of NCAM in spine dynamics and synaptogenesis. Adv. Exp. Med. Biol. 663, 245–256.
Nagy, D., Kocsis, K., Fuzik, J., Marosi, M., Kis, Z., Teichberg, V.I., Toldi, J., Farkas, T., 2011. Kainate postconditioning restores LTP in ischemic hippocampal CA1: onset-dependent second pathophysiological stress. Neuropharmacology 61, 1026–1032.
Pogue, A.I., Cui, J.G., Li, Y.Y., Zhao, Y., Culicchia, F., Lukiw, W.J., 2010. Micro RNA-125b (miRNA-125b) function in astrogliosis and glial cell proliferation. Neurosci. Lett. 476, 18–22.
Prentice, H.M., Moore, S.E., Dickson, J.G., Doherty, P., Walsh, F.S., 1987. Nerve growth factor-induced changes in neural cell adhesion molecule (N-CAM) in PC12 cells. EMBO J. 6, 1859–1863.
Ramsden, M., Kotilinek, L., Forster, C., Paulson, J., McGowan, E., SantaCruz, K., Guimaraes, A., Yue, M., Lewis, J., Carlson, G., Hutton, M., Ashe, K.H., 2005. Age-dependent neurofibrillary tangle formation, neuron loss, and memory impairment in a mouse model of human tauopathy (P301L). J. Neurosci. 25, 10637–10647.
Ronn, L.C., Hartz, B.P., Bock, E., 1998. The neural cell adhesion molecule (NCAM) in development and plasticity of the nervous system. Exp. Gerontol. 33, 853–864.
Rose, S.P., 1996. Cell adhesion molecules and the transition from short- to long-term memory. J. Physiol. Paris 90, 387–391.
Saura, C.A., Choi, S.Y., Beglopoulos, V., Malkani, S., Zhang, D., Shankaranarayana Rao, B.S., Chattarji, S., Kelleher 3rd, R.J., Kandel, E.R., Duff, K., Kirkwood, A., Shen, J., 2004. Loss of presenilin function causes impairments of memory and synaptic plasticity followed by age-dependent neurodegeneration. Neuron 42, 23–36.
Schmid, R.S., Graff, R.D., Schaller, M.D., Chen, S., Schachner, M., Hemperly, J.J., Maness, P.F., 1999. NCAM stimulates the Ras-MAPK pathway and CREB phosphorylation in neuronal cells. J. Neurobiol. 38, 542–558.
Sethi, P., Lukiw, W.J., 2009. Micro-RNA abundance and stability in human brain: specific alterations in Alzheimer's disease temporal lobe neocortex. Neurosci. Lett. 459, 100–104.
Sherrington, R., Rogaev, E.I., Liang, Y., Rogaeva, E.A., Levesque, G., Ikeda, M., Chi, H., Lin, C., Li, G., Holman, K., Tsuda, T., Mar, L., Foncin, J.F., Bruni, A.C., Montesi, M.P., Sorbi, S., Rainero, I., Pinessi, L., Nee, L., Chumakov, I., Pollen, D., Brookes, A., Sanseau, P., Polinsky, R.J., Wasco, W., Da Silva, H.A., Haines, J.L., Perkicak-Vance, M.A., Tanzi, R.E., Roses, A.D., Fraser, P.E., Rommens, J.M., St George-Hyslop, P.H., 1995. Cloning of a gene bearing missense mutations in early-onset familial Alzheimer's disease. Nature 375, 754–760.
Smith, P.Y., Delay, C., Girard, J., Papon, M.A., Planel, E., Sergeant, N., Buee, L., Hebert, S.S., 2011. MicroRNA-132 loss is associated with tau exon 10 inclusion in progressive supranuclear palsy. Hum. Mol. Genet. 20, 4016–4024.
Sun, L.H., Ban, T., Liu, C.D., Chen, Q.X., Wang, X., Yan, M.L., Hu, X.L., Su, X.L., Bao, Y.N., Sun, L.L., Zhao, L.J., Pei, S.C., Jiang, X.M., Zong, D.K., Ai, J., 2015. Activation of Cdk5/p25 and tau phosphorylation following chronic brain hypoperfusion in rats involves microRNA-195 down-regulation. J. Neurochem. 134, 1139–1151.
Tan, L., Yu, J.T., Liu, Q.Y., Tan, M.S., Zhang, W., Hu, N., Wang, Y.L., Sun, L., Jiang, T., Tan, L., 2014. Circulating miR-125b as a biomarker of Alzheimer's disease. J. Neurol. Sci. 336, 52–56.
Wang, W.X., Huang, Q., Hu, Y., Stromberg, A.J., Nelson, P.T., 2011. Patterns of microRNA expression in normal and early Alzheimer's disease human temporal cortex: white matter versus gray matter. Acta Neuropathol. 121, 193–205.
Watanabe, T., Yamagata, N., Takasaki, K., Sano, K., Hayakawa, K., Katsurabayashi, S., Egashira, N., Mishima, K., Iwasaki, K., Fujiwara, M., 2009. Decreased acetylcholine release is correlated to memory impairment in the Tg2576 transgenic mouse model of Alzheimer's disease. Brain Res. 1249, 222–228.
Weingarten, M.D., Lockwood, A.H., Hwo, S.Y., Kirschner, M.W., 1975. A protein factor essential for microtubule assembly. Proc. Natl. Acad. Sci. U. S. A. 72, 1858–1862.
Wemmie, J.A., Chen, J., Askwith, C.C., Hruska-Hageman, A.M., Price, M.P., Nolan, B.C., Yoder, P.G., Lamani, E., Hoshi, T., Freeman Jr., J.H., Welsh, M.J., 2002. The acid-activated ion channel ASIC contributes to synaptic plasticity, learning, and memory. Neuron 34, 463–477.
WHO, 2016. Dementia fact Sheet. Vol., ed.-eds. http://www.who.int/mediacentre/factsheets/fs362/en/.
Wu, C.C., Lien, C.C., Hou, W.H., Chiang, P.M., Tsai, K.J., 2016. Gain of BDNF function in engrafted neural stem cells promotes the therapeutic potential for Alzheimer's disease. Sci. Rep. 6, 27358.
Wu, P., Shen, Q., Dong, S., Xu, Z., Tsien, J.Z., Hu, Y., 2008. Calorie restriction ameliorates neurodegenerative phenotypes in forebrain-specific presenilin-1 and presenilin-2 double knockout mice. Neurobiol. Aging 29, 1502–1511.
Yan, L., Li, L., Han, W., Pan, B., Xue, X., Mei, B., 2013. Age-related neuropsychiatric symptoms in presenilins conditional double knockout mice. Brain Res. Bull 97, 104–111.
Yang, Y., Han, C., 2010. GDNF stimulates the proliferation of cultured mouse immature Sertoli cells via its receptor subunit NCAM and ERK1/2 signaling pathway. BMC Cell Biol. 11, 78.
Yao, P.J., Zhu, M., Pyun, E.I., Brooks, A.I., Therianos, S., Meyers, V.E., Coleman, P.D., 2003. Defects in expression of genes related to synaptic vesicle trafficking in frontal cortex of Alzheimer's disease. Neurobiol. Dis. 12, 97–109.
Yew, D.T., Li, W.P., Webb, S.E., Lai, H.W., Zhang, L., 1999. Neurotransmitters, peptides, and neural cell adhesion molecules in the cortices of normal elderly humans and Alzheimer patients: a comparison. Exp. Gerontol. 34, 117–133.